A Methodology for Detecting Blood-based Abnormalities in Wireless Capsule Endoscopy Videos

Alexandros Karargyris[1] and **Nikolaos Bourbakis** [1, 2]
[1]Wright State University, Engineering College, ATRC, Dayton, OH
[2]AIIS Inc, Dayton OH

Abstract: ***This paper deals with a novel methodology for automatically detecting blood based abnormalities (Bleeding, Angioectasia and Erythema) in Wireless Capsule Endoscopy videos. The methodology is based on a synergistic integration of methods, such as Color K-L transformation, fuzzy region segmentation, Local-Global graphs. The methodology presents several unique features that separate it from the classical bleeding based methods. These features are mainly based on (i) the classification of the blood based pathological cases in three major categories approved by gastroenterologists; (ii) it is based on a synergy of methods tested in the research field for their robustness. Illustrative examples from the methodology are also presented in this paper.***

Keywords: *Wireless capsule Endoscopic Imaging, Processing and Color transformations, Blood Abnormalities, L-G Graphs.*

I. INTRODUCTION

Wireless Capsule Endoscopy is a recently established technology to help physicians identify gastrointestinal diseases and abnormalities in the human small intestine [16]. In the US, so far there has been only one available capsule technology having been distributed by Given Imaging Ltd. © [1, 14, 15]. Besides the capsule itself, physicians are supplied with a software package (RAPID software ©) to view the 8-hour video feedback taken from a patient's digestion tract. In addition to the viewing option, the software offers a limited ability to identify frames with bleeding. However, the results produced by this method are inefficient (72% sensitivity and 85% specificity [2]) leaving the detection of bleeding regions in the small intestine still an open and crucial issue. Moreover, a good detection classification approach of the blood based abnormalities in the intestine is missing by the techniques used in this research area according to the gastroenterologists. Thus, this paper offers a novel approach to automatically detect and categorize blood based abnormalities in the intestine by starting with their definitions.

1.1 DEFINITIONS

Blood-based abnormalities in the small bowel are characterized in three categories: a) Bleeding, b) Angioectasia and c) Erythema. Such a categorization is important in order to comprehend the problem efficiently.

A. Bleeding

Bleeding is defined as the flow of blood from a ruptured blood vessel into the digest tract. Among malignant tumors, leiomyosarcoma is most commonly associated with bleeding. Bleeding with adenocarcinoma is less frequent, and rarely occurs with carcinoid tumors [3].
An inside view of the digestion tract is necessary to reveal possible bleedings. This can be feasible by using Wireless Capsule Endoscopy technology, which is a non-invasive and painless procedure compared to conventional endoscopic procedures like gastrointestinal procedure and enteroscopy. In a multicenter research by Pennazio et al, [4], 29 of the 60 patients underwent push enteroscopy in addition to capsule endoscopy. Among those 29 patients, push enteroscopy detected a source of bleeding in 8 patients (28%), whereas capsule endoscopy detected a source of bleeding in 17 patients (59%).

B. Angioectasia

In medical bibliography angioectasia is also referred to as arteriovenous malformations. It is the most common abnormality accounting for obscure gastrointestinal bleeding, seen in 21%–53% of patients who undergo capsule endoscopy [5]. This makes their detection an important task. They occur more frequently with increasing age and can be identified at endoscopy as spiderlike lesions [6]. Since most of angioectasia cases in small intestine are caused by blood vessels inside the intestine walls. In comparison with bleeding cases, angioectasia stays inside the intestine walls. The color of an angioectasia appears often more reddish than the color of a bleeding.

C. Erythema

In general, erythema is defined as skin redness caused by capillary congestion. In the small intestine erythema multiform is strongly related with various abnormalities (i.e. Croehn's disease). It is an acute, self-limiting, inflammatory skin eruption. Its redness is lesser than that of angioectasia.
An overview of the three cases is presented below (Fig. 1).

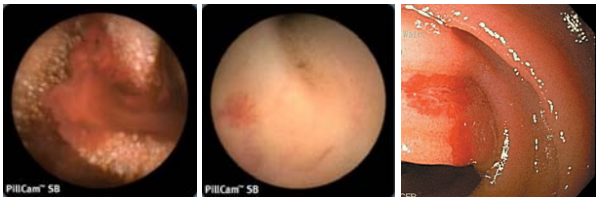

Figure 1. Blood-based abnormalities: Bleeding (left), Erythema (middle), Angioectasia (right)

1.2 PRIOR WORK

In the academics, several research works have been carried out to detect bleeding regions.

In [7], the authors used clotted blood for bleeding. Although their technique aims to detect bleeding regions, it eventually detects blood regions. In their work the 2D color distributions show a significant overlapping of non-blood and blood pixels, though they claim the opposite. In addition, as stated above, a simple examination of the bleeding pixels and non-bleeding pixels can prove that their values are identical in many cases. Dismissing dark pixels from the image doesn't necessary imply removal of non-blood pixels. There are cases when the illumination of the WCE is low making bleeding regions darker. Their methodology dismisses small detected blood regions. It is needless to mention of the existence of small-sized bleeding regions. However, the use of Expectation Maximization clustering and Bayesian Information Criterion are very promising tools, offering an automatic clustering and a statistical approach to this difficult problem.

In [6], the authors proposed applying first color adaptation to the RGB images, which offers image enhancement but the lack of sufficient results and statistics do not justify the efficiency of their methodology. In addition as mentioned before, the R component in WCE images is spread almost at all pixels at high values.

In [8], HSV color space is used to enhance WCE image so that bleeding regions can be extracted easier. It is true that bleeding areas appear better with high color saturation but as the authors state themselves most of the GI tract presents a red dominant color and for highly illuminated GI tract images; the saturation may take very high values making distinction between bleeding and non-bleeding regions impossible. Although their methodology is supposed to consist of multiple features, only saturation and intensity of color are used on step 1 and step 2, which can be further unified into one. In addition the use of multiple and numerous empirical thresholds in step 1 and step 2 makes the methodology less reliable and robust.

II. THE DETECTION METHODOLOGY

The methodology proposed here is based on a synergy of techniques for accomplishing its results.

2.1 METHODOLOGY SYNOPTIC DIAGRAM

In the following diagram we synopsize the sequence of the techniques used in our detection methodology (fig. 2):

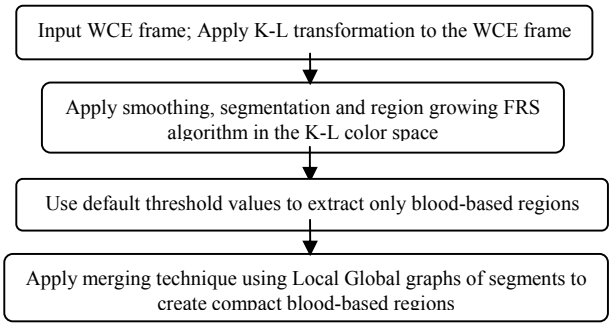

Figure 2: Detection methodology synopsis

2.2 COLOR TRANSFORMATION SCHEME

One could argue that since bleeding regions in WCE images have dominant R component in the RGB color space, their identification must be an easy task. However, this is not the case. After a quick examination, one could easily see that most WCE image pixels carry high values of R, thus dismissing this assumption. It is necessary that other methods must be utilized to approach this problem.

We know that R, G, and B components are highly correlated (Fig. 3). We need to make the input feature space as much uncorrelated as possible so that more useful information can be extracted. That's the reason why in image processing area other color spaces are widely tried and used.

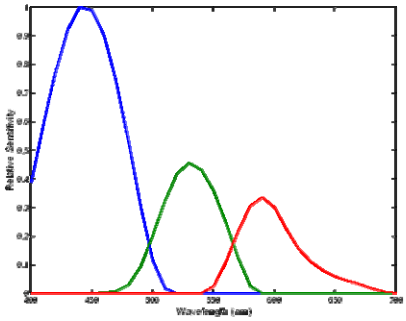

Figure 3. CCD Color Spectral responses for Red, Green and Blue Component

Keeping in mind that RGB color space doesn't offer the visualization ability to enhance and make bleeding regions distinguishable, we tried some major color spaces like HSV, Lab, Luv, YDbDr and CIE-XYZ. YDbDr produced some interesting results but even those didn't prove to be satisfactory. (Fig. 4)

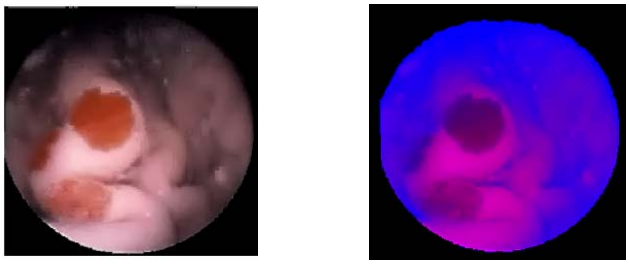

Figure 4. Original WCE image (left) in RGB color space and in YDbDr color space (right)

Thus, a solution is coming from the work of Yu-Ichi Ohta et al, [9]. In their paper, the authors produced a set of color features using Karhunen Loeve transformation of R, G, B components after having evaluated 8 different types of natural images.

The usefulness of a color feature is greatly influenced by the structure of color scenes to be segmented. This statement forced us to investigate the Karhunen-Loeve transformation in our case.

It is well known that R, G and B components overlap in the frequency domain (Fig. 3) and so being highly correlated. Therefore, the need for a transform that can make the R, G, B vectors as much uncorrelated as possible is obvious. We can

remove correlations between pixels using an orthogonal linear transform called Karhunen Loeve transformation [9].

The choice of a linear transformation like Karhunen-Loeve is intentional**.** As mentioned in the work of Kender [11], linear color space transformations are more preferable than non-linear ones for the following reasons:

1) non-linear transforms suffer from non-removable singularities
2) their values are distributed in such way creating spurious modes and gaps and
3) non-linear transforms have higher computational complexity.

On curved surfaces the intensity often gradually changes and cannot be used as a useful feature for segmentation. Color information in natural scenes is almost two dimensional (intensity and one chromatic feature).

In pattern recognition a feature is said to have large discriminant power if its variance is large. Thus, we tried to derive color features (color space) with large discriminant power. More specifically, as described in [9], let S be the region to be segmented and Σ be the covariance matrix of the distributions of R, G and B in S. Let λ1, λ2 and λ3 be the eigenvalues of Σ and $\lambda 1 \geq \lambda 2 \geq \lambda 3$. Let $Wi = (W_{Ri} W_{Gi} W_{Bi})^t$ for i=1,2,3 be the eigenvectors of Σ corresponding to λi, respectively. The color features X1, X2, X3 are defined as:

$$Xi = W_{Ri} \cdot R + W_{Gi} \cdot G + W_{Bi} \cdot B \quad (\|Wi\| = 1,\ i=1,\ 2 \text{ and } 3)$$

It is well known in mathematics that the derived X1, X2 and X3 vectors are uncorrelated.

After many experiments the authors reached to the conclusion that W1 is dominated by $(1/3\ \ 1/3\ \ 1/3)^t$, W2 is dominated by $(1/2\ \ 0\ \ -1/2)^t$ or $(-1/2\ \ 0\ \ 1/2)^t$ and W3 is dominated by $(-1/4\ \ 1/2\ \ -1/4)^t$.

Note that from our experiments we have concluded that W2 = (1 0 -1) gives us better discriminant power.

2.2 Fuzzy Region Segmentation

Segmentation scheme is based on previous work [12]. Here a brief presentation is given. In figure 5 the whole segmentation process is given graphically.

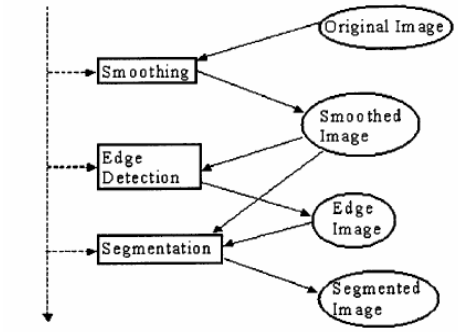

Figure 5. Fuzzy Region Segmentation

Initially a smoothing operation is applied to remove noise from the frame. This operation attempts to preserve the location of edges by only smoothing areas where local contrast (within a small neighborhood) is fairly low. Edge information is utilized from the smoothed input image. The segmentation algorithm uses edge information and the smoothed image to find segments.

The processes involved in this segmentation procedure are as follows.

Edge detection step creates segments that are surrounded by edge pixels or the image boundary. A solid segment is defined as a set of pixels completely surrounded by edge pixels belonging to only one object. To find a solid segment, the image is first scanned for the first non-edge pixel. This pixel is used as a growing seed. In the growing process, a pixel can grow recursively in four directions (left, right, up and down), and merged with the seed if the growing condition is met.

When the growing process ends, if the grown segment is not sufficiently large (i.e. consisting of a threshold quantity of pixels as determined by the image's frequency histogram), the segment is removed. This removal is due to the assumption that the segment found may actually be a part of a larger segment, but was falsely separated because of noise. The weighted average color of the segment is computed, and then the segment is painted with this color.

Next comes the expansion of the big solid matte segments found during the previous phase. The expansion procedure is performed within three sub-phases, during which, the segments are enlarged to include matte pixels with the already delineated matte segments. Larger segments are expanded first. During these sub-phases, each segment is expanded (surrounding pixels merged with the segment) only if the resultant segment is homogeneous. Homogeneity degree is defined as a fuzzy term is *high* if:

1. The absolute similarity (similarity between a pixel's color and the segment's color) is *high*

$$|C(Pn) - C(Ri)| > \tau 1 \text{ and/or}$$

2. The local or relative similarity (similarity between the next and the previous pixel's color in the growing direction) is *high*

$$|C(Pi,j) - C(Pi,j\pm 2)| > \tau 2 \quad or \quad |C(Pi\pm 2,j) - C(Pi,j)| > \tau 3$$

where $C(Pn)$ is the color of current points, and $C(Ri)$ is the color of the region τ1, τ2 and τ3 are selected thresholds. This condition is added to include areas that gradually change in shade while avoiding crossing the object boundary. Color contrast can be measured by computing the difference between two color vectors and obtaining its magnitude. As shown in Eq. (1), the square of the Euclidean distance is used to calculate the color contrast between two-color vectors *v* and *w* in this approach:

$$Contrast\ (v,w) = (Rv - Rw)^2 + (Gv - Gw)^2 + (Bv - Bw)^2 \quad (1)$$

where *R*, *G* and *B* are the three-colour components (Red, Green and Blue). Similarity membership functions are calculated using the equation shown in figure 6.

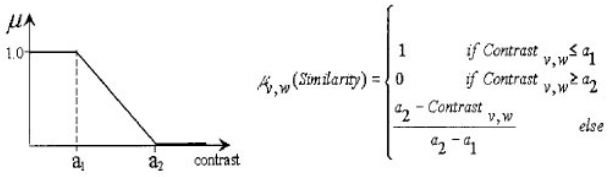

Figure 6. Similarity membership function

Farness measure is used to further expand segments. An unassigned pixel can be close (not far) to a neighboring segment in two senses: 1) close in the spatial domain (physically close); or 2) close in the cluster domain of the color cube (almost of the same color). The degree of farness of a pixel to a neighboring segment

is defined as a product of these two measures. Specifically, the degree of farness for any given pixel is the absolute color contrast multiplied by the geometric distance (in pixels) between the given pixel and the segment border. During this expansion, the degrees of farness for a candidate pixel are computed for its three most closely neighboring segments. The closest segment to the pixel is the one having the lowest degree of farness. If this lowest value belongs to the expanding segment, and is lower than a fixed threshold, the pixel is merged with that segment.

It can be argued that textural measures can help and increase the efficiency in extracting bleeding regions. We tried entropy, contrast, homogeneity, angular moment and correlation features in extracted bleeding regions. Although bleeding regions had similar values in entropy and homogeneity, these values were spread across other non-bleeding regions of WCE frames. This may be caused because of the distribution of pixel values of WCE images, which as mentioned before, are very similar in all regions.

2.3 Local Global Graph

The shape of an object in an image can be described using graph methods. The purpose of these methods is to try to model the geometry of objects in mathematical forms. Having accomplished this, it is much easier to extract useful information of the objects. The Local Global (L-G) graph is such a method (fig. 7). The main components of the L-G graph are:

1. The local graph that represents the information related with color, texture, shape, size etc.
2. The skeleton graph that provides information about the internal shape of each segmented region
3. The global graph that represents the relationships among the segmented regions for the entire image

Thus, the basic idea behind this graph based method is the local and global geometric representation of the image features and their relationships. The selection of the graph structure for representing the information extracted from an image is important for two reasons:

i) It is a generic and very flexible information representation scheme

ii) It is very robust and computationally not very expensive

It is well known that humans visually observe the environment and extract main features or landmarks and inter-relate them for a better representation in their minds.

From the three components mentioned above, we can see that component 1 includes not only geometric information but also color and texture. First, this has to be noted for future reference and secondly, it emphasizes the generality of this method.

The Region or Local Graph holds information of a contour – line of an image region after segmentation.

$G = N_1\ a^c_{12}\ N_2\ a^c_{23.....}\ N_k\ a^c_{k1}N1 \lozenge N_i\ a^p_{ij}\ N_j \lozenge ..... \lozenge N_n\ a^{rd}_{nm}\ N_m$

where ◊ represents the graph relationship operator, and each Ni maintains the structural features of the corresponding line segment, thus, Ni = {sp, orientation (0), length (le), curvature (cu)}, and a_{ij} holds the relationships among these line segments, thus, aij = {connectivity (c), parallelism(p), symmetry (s), relative magnitude (rm), relative distance (rd), etc. }

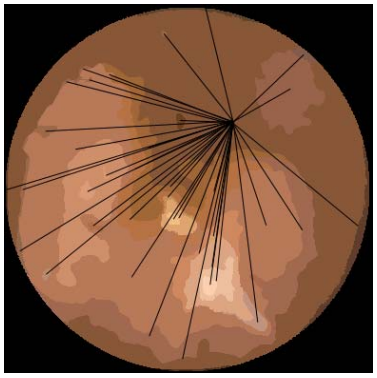

Figure 7. Global graph representation for a single region

The skeleton Graph is part of the L-G graph offering additional information about the regions and is based on the efficient generation of the regions skeletons after the regions segmentation process. The line segments of the skeleton of a region are interrelated with each other through a graph with attributes in a similar way with the one generated by the contour of a segmented region. Thus, the skeleton graph of a region's skeleton is

$G = K_1\ a^c_{12}\ K_2\ a^c_{23.....}\ K_k\ a^c_{kq}Nq \lozenge K_i\ a^p_{ij}\ K_j \lozenge ..... \lozenge K_n\ a^{rd}_{nm}\ K_m$

where ◊ represents the graph relationship operator, and each Ki maintains the structural features of the corresponding line segment, thus, Ki = {sp, orientation (o), length (le), curvature (cu)}, and aij holds the relationships among these line segments, thus, aij = {connectivity (c), parallelism (p), symmetry (s), relative magnitude (rm), relative distance (rd), etc.}. The missing elements for a global visual perception of an image are: the color (or texture) of each region, its relative geographic location (distance and angle) among the other regions, its relative size in regards with the other regions, etc. One way to obtain these additional features is the development of the global image graph GG.

The image Global Graph (GG) attempts to emulate a human-like understanding by developing global topological relationships among regions and objects. More specifically, for each image region Mi, a skeletonization task is performed and the final centroid GCg(i,x,y) is defined. When all the final centroids have been defined for every image region, the global image graph is developed:

GG(Ak) = (P1R12P2)Φ23(P1R13P3)…(P1R1n-1Pn-1)Φn-1n (P1R1nPn)

where Pi is a node that represents an image region graph, its color, and its GCg(i,x,y), Rij represents the relative distance between two consecutive GCg, and the orientation of each dg, Φij represents the relative angle between consecutive distances dg(i) and dg(j). An important feature of the L-G graph is its ability to describe 3-D scenes. The only difference between 2-D from 3-D is that in 3-D the local graph will represent 3-D surfaces and the global graph will appropriately interrelate them.

Region Synthesis [13]

The synthesis of regions is an important step that leads to patterns or objects recognition. The Local-Global graph method used here can match a pattern or an object with deformation other than rigid transformation. However, it assumes that the shape has been segmented from the background, and the mathematical shape representation is sensitive to some kinds of deformations, for example, if the shape of a region changes the local graph and the skeleton graph record the changes attached them to the L-G graph.

In addition, the centroid may change and the global graph will register that change as well. The process used here for objects recognition is based on the synthesis of segmented adjacent regions, using the L-G graph, and association (comparison) of the integrated region models available in a database. Figure 8 shows the synthesis of the regions based on the L-G graph. Figure 9 presents the synthesis of the regions selected in 5 steps for the generation of a new region that the physician will consider it as one. Note that the final region regains the RGB values of its pixels.

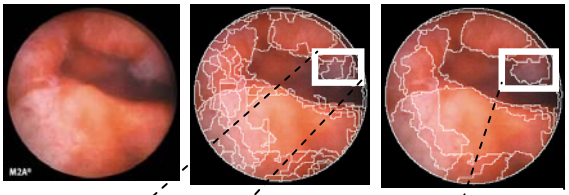

Figure 8. Original image and Segmentation with Region Merging / Synthesis

Figure 9. Spatial Connectivity Graph for Synthesis of the marked area of figure 8.
The merged regions regain their original RGB values

Figure 10 presents an example of the methodology.

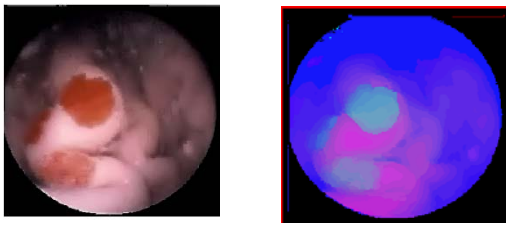

Figure 10. Original WCE image with bleeding regions (left) and the same image in the designed K-L Color feature space (right)

III. SOME EXPERIMENTAL RESULTS

We tested our methodology using images available in the RAPID Atlas ® which is a library of reference images, offered by Given Imaging ©.

Some identified bleeding regions frames are shown in figure 11. The algorithm offers the option to give the number of bleeding pixels as well as the percentage of bleeding in the given frame, so that the physician has better understanding of the seriousness of the case.

Angioectasia

Erythema

Bleeding

Figure 11. Blood-based abnormalities are marked with black outline

It is important to be mentioned that the methodology should identify regions that may be suspicious even though after physician's examination, are proved not to be. This is a desirable feature that gastroenterologists want present in any automated software methodology.

A large scale testing with various blood-based frames is in progress in co-ordinance with a professional gastroenterologist so that useful statistics regarding the specificity and sensitivity of the methodology can be acquired.

The methodology was developed in a GUI under MFC in C++ for easier compatibility. The software can run both in Microsoft© Windows XP© Service Pack 2 and the newer version Microsoft© Windows Vista© Service Pack 1.

IV. CONCLUSION

In this paper a new methodology was proposed for extracting bleeding regions in WCE frames based on the orthogonal Karhunen –Loeve transform. We are planning a large scale testing for detecting blood-based abnormalities while enabling the algorithm to categorize the detected regions into the three major categories discussed in section 1. In addition, we are in a stage to implement a preprocessing scheme that will enhance WCE images before applying the detection algorithm. We are confident that this will improve the total efficiency.

Local Global (LG) Graph scheme proved to be a powerful tool in our methodology since it offered us with the power of geometry description of extracted blood-based regions. Having this "description" in our hands we were able to merge smaller regions into bigger solid ones using synthesis method. In addition the LG

graph scheme is enabling us to use the geometric and color characteristics of the regions in order to categorize the abnormalities more efficiently.

A comparative study is in progress to evaluate the performance and robustness of the method proposed here by selecting a set of WCE videos from the Digestive Associates Inc. ®. The evaluation of the method will be not only with results on successful cases versus other methods, but an actual approval by the Digestive Associates medical team.

Future research work is aimed at identifying different abnormalities like polyps and ulcers in WCE videos

Acknowledgment

This work is partially supported by AIIS Inc. The authors express their appreciation to Dr. M. Pouagare, MD, Digestive Associates Inc. ®, for his valuable advices and evaluation during the testing of our methodology.

V. REFERENCES

[1] Given Imaging Ltd., http://www.givenimaging.com

[2] S. Liangpunsakul, L. Mays and DK Rex. "Performance of Given suspected blood indicator" American Journal of Gastroenterology, Vol. 89. No. 12, 2003

[3] Ramirez F. Gastroenterology and Hepatology: Small Intestine. Ed. by Mark Feldman (series editor), Lawrence R. Schiller. ©1997 Current Medicine Group LLC.

[4] Pennazio M, Santucci R, Rondonotti E, et al. Wireless capsule endoscopy in patients with obscure gastrointestinal bleeding: Results of the Italian multicenter experience. Gastrointestinal Endoscopy 2002; 55:AB87

[5] Hara AK, Leighton JA, Sharma VK, Fleischer DE. Small bowel: preliminary comparison of capsule endoscopy with barium study and CT. Radiology 2004; 230:260–265

[6] Radiological Society of North America, Radiographics Journal, *Imaging of Small Bowel Disease: Comparison of Capsule Endoscopy, Standard Endoscopy, Barium Examination, and CT*, http://radiographics.rsnajnls.org/cgi/content/full/25/3/697#F3A , Article viewed in May 2008.

[7] S. Hwang, J. Oh, J. Cox, S. J. Tang, and H. F. Tibbals. Blood detection in wireless capsule endoscopy using expectation maximization clustering, volume 6144. SPIE, 2006.

[8] P.Y. Lau, P. L. Correia, "Detection of Bleeding Patterns in WCE Video using Multiple Features", Proceedings of the Int.
Conf. of the IEEE Engineering in Medicine and Biology Society, EMBC'2007, Lyon, France, Aug. 2007

[9] Y. Ohta, T. Kanade, and T. Sakai, "Color Information for Region Segmentation," Computer Graphics and Image Processing, Vol. 13, No. 3, July, 1980, pp. 222 - 241.

[10] Applied and Computational Control,. Signals, and Circuits—Volume 1, edited by Biswa Nath Datta, Birkhäuser,. 1999, 539 pp., ISBN 0-8176-3954-3

[11] J. Kender, Saturation,Hue and Normalized Color: Calculation, Digitization Effects and Use, Technical Report, Dept of CS, Carnegie-Mellon University, 1976.

[12] Moghaddamzadeh, A. and Bourbakis, N., A fuzzy region growing approach for segmentation of color images. Pattern Recognition. v30 i6. 867-881.

[13] N. Bourbakis, Detecting abnormal patterns in WCE images, IEEE Symp. BIBE-05, Oct. 17-19, 2005, MN, pp. 232-238.

[14] Jamie S. Barkin, Wireless Capsule Endoscopy, Gastrointestinal Endoscopy Clinics of North America , vol.14,No.1, Jan. 2004

[15] R.De. Francis et. al., Sensitivity and specificity of the red blood identification system (RBIS) in video capsule endoscopy, 3rd Int. Conf. on Capsule Endoscopy, Feb. 2004, Miami, FL, USA.

[16] A. Karargyris and N. Bourbakis, A Survey on WCE Imaging Systems and Techniques, IEEE Engineering in Medicine and Biology, to appear

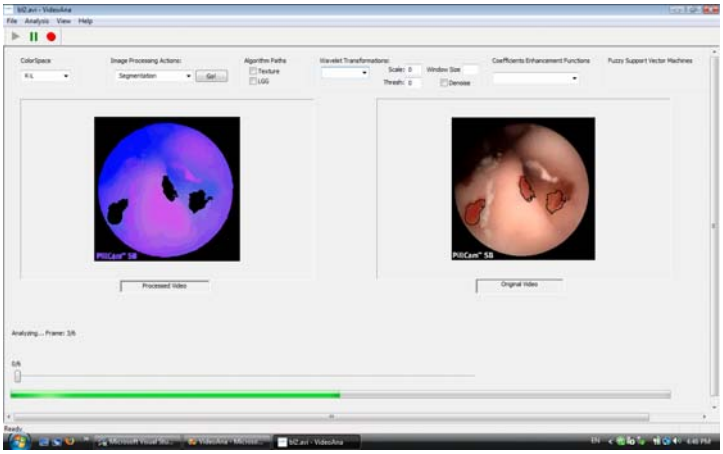

Figure 11. ATRC VideoAnalysis Toolbox